A thermodynamic study of mesophilic, thermophilic, and hyperthermophilic L-arabinose isomerases: The effects of divalent metal ions on protein stability at elevated temperatures

Dong-Woo Lee[a,b], Young-Ho Hong[a], Eun-Ah Choe[a], Sang-Jae Lee[a], Seong-Bo Kim[a], Han-Seung Lee[b], Jong-Won Oh[a], Hae-Hun Shin[c], Yu-Ryang Pyun[a,*]

[a] *Department of Biotechnology, Yonsei University, Seoul 120-749, Korea*
[b] *Department of Biochemistry and Molecular Biology, University of Georgia, Athens, GA 30602-7229, USA*
[c] *Division of Foodservice Industry, Baekseok College, Cheonan 330-705, Korea*

Received 4 October 2004; revised 18 November 2004; accepted 9 January 2005

Available online 26 January 2005

Edited by Christian Griesinger

Abstract To gain insight into the structural stability of homologous homo-tetrameric L-arabinose isomerases (AI), we have examined the isothermal guanidine hydrochloride (GdnHCl)-induced unfolding of AIs from mesophilic *Bacillus halodurans* (BHAI), thermophilic *Geobacillus stearothermophilus* (GSAI), and hyperthermophilic *Thermotoga maritima* (TMAI) using circular dichroism spectroscopy. The GdnHCl-induced unfolding of the AIs can be well described by a two-state reaction between native tetramers and unfolded monomers, which directly confirms the validity of the linear extrapolation method to obtain the intrinsic stabilities of these proteins. The resulting unfolding free energy (ΔG_U) values of the AIs as a function of temperature were fit to the Gibbs–Helmholtz equation to determine their thermodynamic parameters based on a two-state mechanism. Compared with the stability curves of BHAI in the presence and absence of Mn^{2+}, those of holo GSAI and TMAI were more broadened than those of the apo enzymes at all temperatures, indicating increased melting temperatures (T_m) due to decreased heat capacity (ΔC_p). Moreover, the extent of difference in ΔC_p between the apo and holo thermophilic AIs is larger than that of BHAI. From these studies, we suggest that the metal dependence of the thermophilic AIs, resulting in the reduced ΔC_p, may play a significant role in structural stability compared to their mesophilic analogues, and that the extent of metal dependence of AI stability seems to be highly correlated to oligomerization.

Keywords: L-Arabinose isomerase; Unfolding; Heat capacity; Metal ion; Structural stability

1. Introduction

Hyperthermophiles that can survive in harsh environments, and their thermostable enzymes, have been extensively studied to understand the basis of thermostabilization and/or thermal adaptation [1–3]. To reveal the main strategies used for protein stabilization, numerous three-dimensional structures of themophilic proteins have been obtained in order. Comparative studies of thermophilic and mesophilic enzymes have demonstrated that weak interactions such as hydrogen bonds [4], disulfide bonds [5], ion pairs [6], salt bridges [7], hydrophobic interactions [8], and compactness [9] are of importance for stability. However, no universal basis of stability has been recognized because the stability of different enzymes has different origins. For this reason, more extensive studies have been performed to elucidate the fundamentals of protein stability in terms of macromolecular interactions based on thermodynamics [10–12].

Equilibrium denaturation studies have provided detailed knowledge of the structure, stabilization, and folding of small, monomeric proteins [13,14]. Thermodynamic comparison of mesophilic and thermophilic ribonuclease H revealed that the heat capacity of unfolding of the thermophilic enzyme is lower than that of its mesophilic counterpart, although the proteins have maximal stabilities at similar temperatures [13]. For two small single-domain CheY homologues from *Thermotoga maritima* and *Bacillus subtilis*, it was found that the enhanced thermostability of the former is a direct result of the increased enthalpy contribution at the temperature of zero entropy, T_s, and the decreased heat capacity change upon unfolding [14]. In addition, the dimeric serine hydroxymethyltransferases from *B. subtilis* and *Geobacillus stearothermophilus* followed different unfolding paths despite having a high degree of sequence identity [15].

Although, a general understanding of the forces involved in protein stability would require investigation of multi-subunit proteins in which additional modes of stabilization are available at the quaternary structural level, structural thermodynamic studies of the unfolding of oligomeric proteins are rare [16,17]. In recent years, it has been reported that between mesophilic and thermophilic proteins, oligomerization is an optional strategy used by evolution [18,19]. However, little comparative thermodynamic data for oligomeric unfolding mechanisms and stability have derived from studies of similar orthologous proteins.

For these and related reasons, we have begun to study the unfolding of bacterial L-arabinose isomerases (AI), specifically the three homo-tetrameric metalloenzymes (M_r = 225 000) from mesophilic *B. halodurans*, thermophilic *G. stearothermophilus*, and hyperthermophilic *T. maritima* that contain 498 residues per monomer [20,21]. Although, these AIs are highly conserved with respect to primary amino acid sequence (similarity, >70%) and secondary structure [20], in contrast to mesophilic AIs such

*Corresponding author. Fax: +82 2 312 6821.
E-mail address: yrpyun@yonsei.ac.kr (Y.-R. Pyun).

0014-5793/$30.00
doi:10.1016/j.febslet.2005.01.027

as *E. coli* AI, *B. halodurans* AI, and *Lactobacillus gayonii* AI, (hyper) thermophilic AIs from *T. maritima* [20], *T. neapolitana* [22], and *G. stearothermophilus* [21] showed an absolute metal dependence for their thermostability as well as active conformation. In addition, they also have metal-mediated isomerization activity not only for arabinose to ribulose in vivo but also for galactose to tagatose in vitro. In recent years, these thermophilic AIs have received considerable attention because of their use for producing the novel sweetener, D-tagatose [23].

Thus, in order to investigate the role of divalent metal ions on thermophilic AIs, we report here studies on isothermal guanidine hydrochloride (GdnHCl)-induced unfolding of metal free- and Mn-containing AIs monitored at equilibrium using circular dichroism (CD) that is sensitive to protein secondary structure. These unfolding studies demonstrate that thermostable AIs mainly have lower heat capacity and higher unfolding energy than their mesophilic counterparts, and that divalent metal ions assume a key role in oligomerization and subsequent AI stability at elevated temperatures, reflecting thermal adaptation of these enzymes.

2. Materials and methods

2.1. Expression and purification of AIs

To express the recombinant enzymes, *E. coli* BL21 cells transformed with pET-BHAI, pET-GSAI, pET-TMAI were grown at 37 °C in 1 liter LB medium containing 100 μg of ampicillin per ml, induced in mid-exponential phase (A_{600} = 0.6) with 1 mM of isopropyl-β-D-thiogalactopyranoside, grown for an additional 5 h, and harvested by centrifugation (10000 × *g*, 20 min, 4 °C).

Recombinant AIs were purified as described elsewhere [20,21]. The purified AIs were dialyzed against 10 mM Tris–HCl buffer [pH 7.0 except with *B. halodurans* (BHAI) at pH 8.0] and stored at 4 °C. Protein concentrations were determined by the bicinchoninic acid method, with bovine serum albumin as standard. Enzyme fractions were analyzed by 12% SDS–PAGE and visualized with Coomassie blue [24].

2.2. Metal content analysis and enzyme preparation

In order to verify the metal content of AIs, column-purified enzymes were rendered metal-free and then reconstituted with pure metals. Metal ions were removed from the purified AIs by treatment with 10 mM EDTA at 25 °C for 3 h followed by overnight dialysis against 10 mM Tris buffer (pH 7.0 or 8.0) at 4 °C with several changes of buffer. Thereafter, the metal-free enzymes were dialyzed against the same buffer containing 1 mM Mn^{2+} to form the metal-substituted enzymes. Divalent metal content of the as-isolated and EDTA-treated samples were determined by high-resolution inductively coupled plasma-mass spectrometry on a PlasmaQuad 3 instrument at the Chemical Analysis Laboratory, University of Georgia.

For AI unfolding experiments, samples containing 0.3 mg/ml EDTA-pretreated protein, 10 mM Tris–HCl (pH 7.0 or 8.0), 1 mM Mn^{2+}, and the appropriate concentration of GdnHCl were allowed to equilibrate overnight before CD measurement. GdnHCl-induced denaturation of AIs was achieved by serial addition of a solution containing a high GdnHCl concentration, 0.3 mg/ml protein, 10 mM Tris–HCl buffer (pH 7.0 or 8.0) into a starting solution containing the above without GdnHCl. The same starting and titrant solutions were used for each protein to measure equilibrium unfolding at eight or nine different temperatures, ranging from 15 to 80 °C. The time necessary to reach equilibrium (1 min to several hours) varied with the protein, denaturant concentration, and temperature. Equilibrium was ensured by monitoring the CD signal over time until no further change was observed.

2.3. Circular dichroism

Circular dichroism (CD) measurements were carried out in a Jasco J-810 spectropolarimeter with a Peltier temperature-controlled cuvette holder. The CD spectra of the enzyme samples (0.3 mg/ml) in 10 mM Tris–HCl buffer (pH 7.0 or 8.0) were recorded at 222 nm. Samples were overlaid with mineral oil and the lids of the cuvettes were sealed with paraffin tape to prevent evaporation. Each CD measurement is the average of the signal over 5 min in a 0.1 cm path length cuvette. Temperature equilibration during isothermal unfolding was ensured by monitoring the CD signal over time until no further change was observed.

2.4. Thermodynamic study

Denaturant-induced unfolding of AI was carried out isothermally in the presence of 10 mM Tris–HCl buffer (pH 7.0 or 8.0) at temperatures ranging from 15 to 80 °C. Changes in ellipticity at 222 nm were monitored by CD spectropolarimetry. The data were fitted by nonlinear least-squares analysis using the linear extrapolation model [25].

To determine the stability curve, we calculated free energies of unfolding (ΔG_U) from the GdnHCl denaturation of the three AIs at several temperatures, assuming a two-state model and a linear relationship between ΔG_U and [GdnHCl] [25,26]. The ratio of denatured and total protein in the transition range, f_d, was evaluated from their signal ε relative to the signals of the native and unfolded baselines, according to the following equation:

$$f_d = (\varepsilon_N - \varepsilon)/(\varepsilon_N - \varepsilon_U) \quad (1)$$

where ε_N and ε_U represent the CD signal of the fully folded and unfolded forms of the protein, respectively, in the transition region. These are functions of denaturant concentration [D] and temperature, and were calculated according to the following equation:

$$\varepsilon_N = \varepsilon_N^0 + m_{N,D}[D] + m_{N,T}T \quad \varepsilon_U = \varepsilon_U^0 + m_{U,D}[D] + m_{U,T}T \quad (2)$$

where ε_N^0 and ε_U^0 represent the intercepts of the folded and unfolded base planes, $m_{N,D}$ and $m_{U,D}$ represent their slopes with respect to denaturant concentration, and $m_{N,T}$ and $m_{U,T}$ represent their slope with respect to temperature.

The relative population of species was transformed to the respective equilibrium constant K_U for a tetramer according to Neet and Timm [27], using the following equation:

$$K_U = 4P_t[f_d^4/(1 - f_d)] \quad (3)$$

where the monomer concentration P_t is in moles per liter.

To calculate free energies of stabilization, Eq. (4) was employed

$$\Delta G_{obsd} = -RT \ln K_U \quad (4)$$

where ΔG_{obsd} is the difference in Gibbs free energy between the folded and unfolded states, where the folded state is the reference state. The free energies of unfolding (ΔG_U) was determined through a series of isothermal curves at different temperatures, assuming a two-state model and a linear relationship between ΔG_{obsd} and [D] (Eq. (5)). Linear extrapolation of the equation to zero denaturant concentration yields the free energy change in the absence of denaturant, $\Delta G_U(H_2O)$:

$$\Delta G_{obsd} = \Delta G_U(H_2O) + m[D] \quad (5)$$

where [D] is denaturant concentration. The term *m* represents the effectiveness of the denaturant in denaturizing the protein and is considered to be independent of denaturant concentration.

Thermal melts were fit to determine the T_m for each protein, using a two-state model [28] and the Gibbs–Helmholtz relationship between ΔG_U and temperature. The resulting free energies of unfolding (ΔG_U) were plotted as a function of temperature. Temperature dependence of ΔG_U can be written as

$$\Delta G_U(T) = \Delta H_U^0 - T\Delta S_U^0 + \Delta C_{p,U}[T - T^0 - T\ln(T/T^0)] \quad (6)$$

where ΔH_U^0 and ΔS_U^0 refer to the enthalpy and entropy of unfolding at the reference temperature T^0, respectively, and $\Delta C_{p,U}$ is the heat capacity of unfolding, assumed to be independent of temperature. T_m is the temperature at which native and unfolded states have the same population. When $\Delta G_U = 0$ (i.e., at the T_m), $\Delta S_U^0 = \Delta H_U^0/T_m$. However, Eqs. (5) and (6) give

$$\Delta G_U(T,D) = \Delta H_U^0 - T\Delta H_U^0/T_m + \Delta C_{p,U}[T - T_m - T\ln(T/T_m)] - m[D] \quad (7)$$

Therefore, using the T_m as the reference temperature, the data (GdnHCl-induced equilibrium unfolding at different temperature) were fit to the modified version of the Gibbs–Helmholtz equation (Eq. (7)) to determine ΔH^0_U, $\Delta C_{p,U}$, and T_m for each protein. The program OriginPro 7 (OriginLab) was used for fitting of the required parameters.

3. Results and discussion

3.1. GdnHCl-induced unfolding of AIs

We investigated the equilibrium unfolding of BHAI, GSAI (*G. stearothermophilus* AI), and TMAI (*T. maritima* AI) by monitoring changes in the intrinsic ellipicity of CD at 222 nm, using GdnHCl as denaturant. Fig. 1A shows the far-UV CD spectra of folded and GdnHCl-unfolded TMAI as an example. The high α-helical content dominates the spectrum of the native protein with the characteristic negative value of the ellipticity at 222 nm, which vanishes upon unfolding. For comparison of the effect of metal ions on protein stability, we also evaluated GdnHCl-induced unfolding of the AIs in the presence and absence of Mn^{2+}. As shown in Fig. 1B, GdnHCl-induced unfolding of BHAI, GSAI, and TMAI at 25 °C, when monitored by changes in secondary structural content, involves highly cooperative transitions between the native and unfolded states, with no detectable intermediates, generating sigmoidal transition curves. The far-UV CD spectrum of native AI displays a minimum around 222 nm. Upon complete denaturation in 6 M GdnHCl, there was a large decrease in CD intensity at 222 nm, indicating loss of secondary structure.

As previously reported, it was found that the metal dependence of the AIs increased with the temperature at which they were assayed [20,21]. To further characterize this aspect, we analysed the decrease in enzyme activity of the apo and holo proteins at various GdnHCl concentrations (Fig. 2A). The activity decay curves showed cooperative transitions similar to the above GdnHCl unfolding profiles. For each of the AIs, the transitions defined by far-UV CD coincided with those derived from enzymatic activity measurements. However, the midpoint concentrations of the activity loss are lower (approximately 0.3–0.5 M) than those of the structural transition as shown in Fig. 1B, probably because the active conformation of a thermophilic AI achieved at elevated temperature could not be detected in the GdnHCl-induced unfolding profiles at room temperature. We previously reported that thermophilic AIs have a metal-mediated active conformation at the elevated temperatures different from their inactive forms at 25 °C, indicating the conformational flexibility of AIs although the protein is folded at both temperatures [21]. Nonetheless, Fig. 2A clearly shows that the active populations of the holo proteins are more stable than those of the apo proteins upon GdnHCl unfolding and that the metal dependence of TMAI and GSAI is higher than that of BHAI. The above results indicate that Mn^{2+} could be more effective for thermophilic AIs than its mesophilic counterpart in maintaining protein stability.

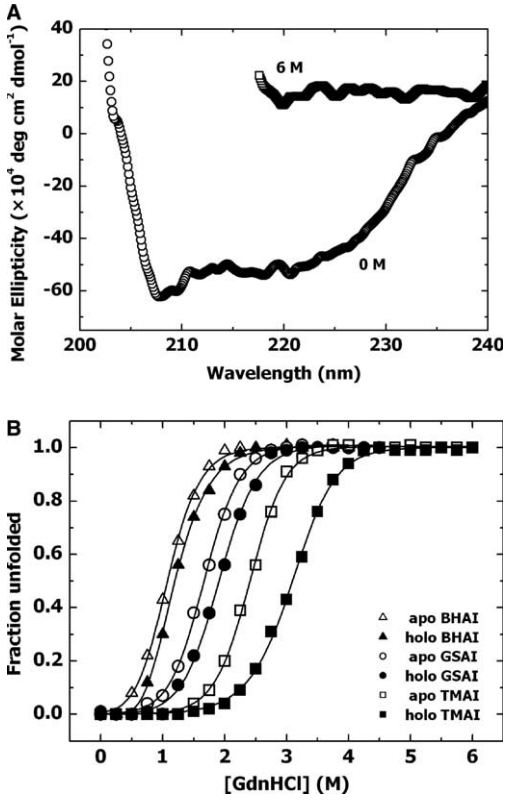

Fig. 1. (A) CD spectra of TMAI in the far-UV region. Numbers represent GdnHCl concentrations. (B) Equilibrium unfolding transitions of metal-free and Mn^{2+}-bound AIs induced by GdnHCl at 25 °C and monitored by CD ellipticity at 222 nm.

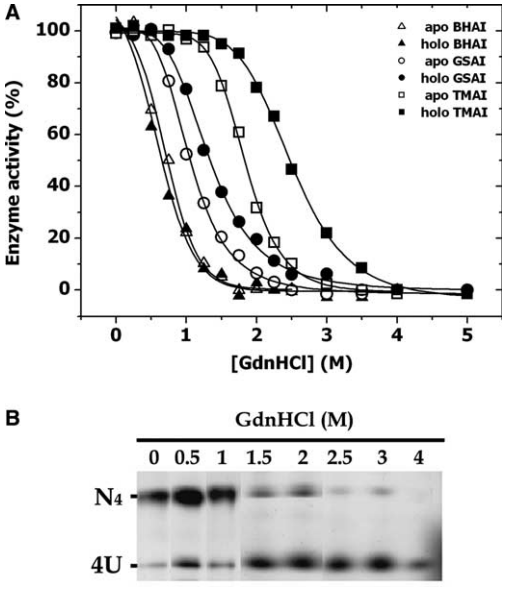

Fig. 2. (A) Loss of enzymatic activity with increasing GdnHCl concentration. Values are percentages of native activity. The reaction mixtures contained 50 mM HEPES buffer (pH 7.0 at room temperature, except with BHAI at pH 8.0), 1 mM Mn^{2+}, 0.1 M L-arabinose, 1 ml of enzyme solution at various [GdnHCl], and distilled water to a final volume of 1.25 ml. Assays of BHAI, GSAI, and TMAI were incubated for 20 min at 50, 70, and 90 °C, respectively, and stopped by cooling on ice. The ribulose formed was determined by the cysteine–sulfuric acid–carbazole method, and the A_{560} measured [29]. One unit of isomerase activity is defined as the amount of enzyme that produces 1 μmol of product per minute under these conditions. (B) GdnHCl-induced changes in subunit configuration during AI unfolding. The representative native-4 to 20% linear gradient PAGE of GdnHCl-treated GSAI under the unfolding conditions.

In order to verify that a two-state model could be used to describe AI unfolding, we performed native-PAGE in the presence of GdnHCl as denaturant (Fig. 2B). Generally, the unfolding equilibrium of homotetrameric proteins can be presented as $N_4 \leftrightarrow 4N\ (I) \leftrightarrow 4U$, where N_4, N (I), and U represent the native oligomer, dissociated monomer (Intermediate), and denatured monomer, respectively. In the present case, however, the intermediate is not likely to be present in a significant amount. This is reflected in Fig. 2B, which provides evidence in support of a two-state model for AI unfolding in various concentrations of GdnHCl. Here, the AIs appear as either extremely stable tetramers or unfolded monomers. From these results, the formation of an intrinsically unstable state(s) or folded monomeric species at equilibrium is unlikely, demonstrating that AI unfolding is linked to subunit dissociation, and that a two-state equilibrium ($N_4 \leftrightarrow 4U$) model could be applied for the AIs. Hence, given the two states of AI conformation, it is possible to apply the linear extrapolation method (LEM) to tetrameric AIs for evaluating the free energy change (ΔG_U) upon conversion of native to unfolded proteins in the absence of denaturant [18,27].

3.2. Linear dependence of ΔG_U on GdnHCl concentration

The observed equilibrium constants evaluated in the transition region in Fig. 1B were converted to free energy values and then plotted as a function of denaturant (Fig. 3). To estimate the free energy change for unfolding in the absence of denaturant, ΔG_U (H_2O), the data were extrapolated to zero denaturant concentration. Assuming a two-state transition and a linear dependence of ΔG_U on GdnHCl [25], the resulting ΔG_U values at 25 °C for the holo proteins of BHAI, GSAI, and TMAI were 57.6, 65.9, and 83.1 kJ/mol, respectively. To investigate the effect of metal ions on protein stability, we also followed GdnHCl-induced unfolding behaviour of the apo AIs under the same conditions. Fig. 3 shows that the differences in slopes between the apo and holo proteins of (hyper)thermophilic AIs are much larger than in their mesophilic counterpart, demonstrating the relative importance of metal ions for thermophilic AIs with respect to the unfolding process and protein stability. However, there was little difference in ΔG_U (H_2O) between the apo and holo proteins for each AI. Using Eq. (5), we can derive denaturant *m* values, i.e., the dependence of free energy of unfolding on denaturant concentration, for the apo and holo proteins of 20.3 and 19.9 kJ/M mol for BHAI, 19.6 and 17.8 kJ/M mol for GSAI, and 19.9 and 16.3 kJ/M mol for TMAI, respectively. The fact that the slopes of the denaturation curves for GSAI and TMAI are much steeper in the case of the apo proteins than of the holo proteins indicates that the amount of protein surface exposed to solvent upon unfolding is larger for the apo proteins [30]. These observations indicate that metal ions cause the thermophilic holo proteins to be less affected by the same amount of GdnHCl than the apo protein, and that thermophilic AIs have significant metal dependence contributing to the maintenance of protein conformation.

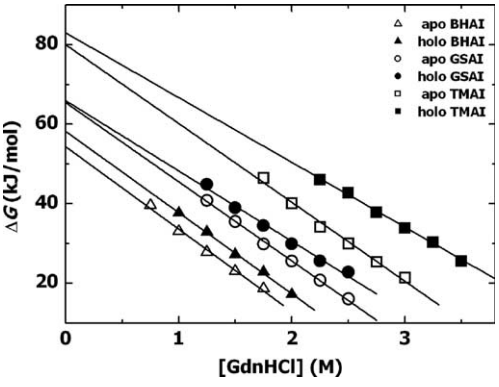

Fig. 3. Unfolding free energy changes as a function of [GdnHCl] at 25 °C. ΔG values were obtained by applying the linear extrapolation model to the GdnHCl-induced unfolding data. The linear extrapolation method equation is: $\Delta G_{obsd} = \Delta G_U(H_2O) + m[\text{GdnHCl}]$ (Eq. (5)).

3.3. Stability curves of BHAI, GSAI, and TMAI

To obtain global stability curves of BHAI, GSAI, and TMAI, we have examined isothermal GdnHCl-induced unfolding of the AIs at several temperatures by circular dichroism. The isothermal unfolding profiles, as shown in Fig. 4A, were fit to the two-state model as described in Experimental. We then calculated the *m* values for each AI over the whole range of temperatures examined (Table 1). The independence of the *m* values from temperature allowed us to fit the data globally in a single and reliable step using a modified Gibbs–Helmholtz equation (Eq. (7)). For each protein, ΔG_U was plotted as a function of temperature, resulting in the protein stability curves shown in Fig. 4B. The stability

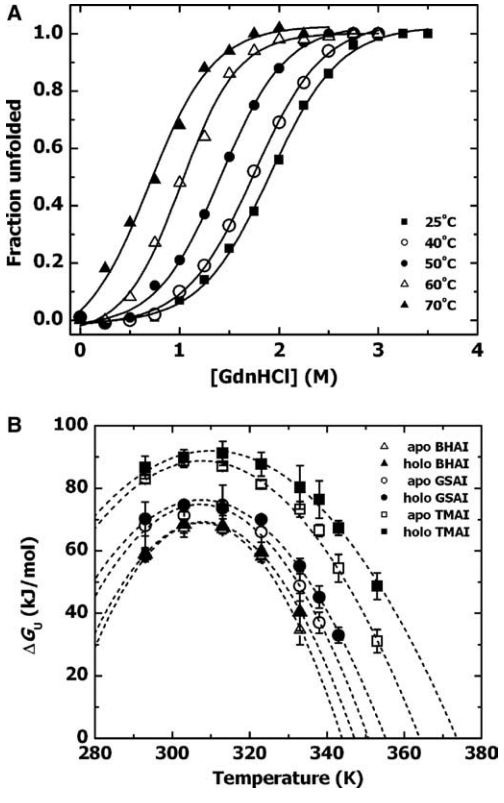

Fig. 4. (A) Equilibrium unfolding transitions of GSAI induced by GdnHCl at several temperatures in the presence of 1 mM Mn^{2+} and monitored by CD ellipticity at 222 nm. (B) Protein stability curves. Each point represents a ΔG_U determined from a GdnHCl-induced isotherm experiment. Lines represent fits to the Gibbs–Helmholtz equation; errors shown are for the fits.

Table 1
Temperature dependence of m values (kJ/mol M) for BHAI, GSAI, and TMAI

Temperature (K)	BHAI		GSAI		TMAI	
	Apo	Holo	Apo	Holo	Apo	Holo
293	21.9 ± 1.6	20.9 ± 1.2	20.1 ± 0.9	18.4 ± 1.1	20.9 ± 0.9	16.3 ± 1.3
303	26.1 ± 8.2	25.4 ± 4.0	23.0 ± 1.1	18.6 ± 1.1	18.3 ± 1.4	13.6 ± 4.2
313	25.0 ± 4.0	24.9 ± 1.9	23.6 ± 3.9	21.9 ± 2.5	18.4 ± 1.1	15.7 ± 2.7
323	22.4 ± 0.8	21.1 ± 2.1	23.3 ± 2.5	22.1 ± 1.3	22.5 ± 2.3	14.3 ± 3.8
333	21.8 ± 1.4	19.6 ± 0.5	21.1 ± 3.9	19.1 ± 4.4	21.4 ± 0.6	18.0 ± 0.8
343	–		–		20.7 ± 1.2	16.6 ± 0.7

The value corresponds to the means ± S.D.

curves were then fit to Eq. (7) to obtain the thermodynamic parameters ΔC_p, ΔH^0, and T_m (Table 2). As shown in Fig. 4B and Table 2, TMAI and GSAI are more stable than BHAI at all temperatures. The T_ms of holo-TMAI and -GSAI are 27 K and 9 K higher than of holo BHAI, and the ΔC_p values of TMAI and GSAI are 2.2- and 1.4-fold lower than of that of BHAI, respectively. Since ΔC_p is related to the temperature dependencies of both ΔS and ΔH, these after two parameters vary less with temperature for TMAI and GSAI than for BHAI, resulting in an increased breadth of the stability curves, or T_m. The differences in ΔC_p for the apo and holo proteins of TMAI and GSAI were 3.8–4.2 kJ mol^{-1} K^{-1}. It is clearly shown that the reduced ΔC_p of the thermophilic AIs contribute to flatten the stability curve resulting in the more increased T_m and higher ΔG_U than that of BHAI (Fig. 4B). Although, the hyperthermophilic TMAI seems to adopt the same strategy in terms of decreased ΔC_p as GSAI, compared to BHAI, this is insufficient to describe the higher protein stability of TMAI. Despite the fact that differences in reduced ΔC_p values for TMAI and GSAI were nearly the same (Table 2), the T_m for hyperthermophilic TMAI was significantly greater than that of thermophilic GSAI, indicating that the reduced ΔC_p of TMAI is not solely responsible for the thermostability of the protein. As shown in Fig. 4B, the stability curve for TMAI was shifted to a much higher ΔG_U at all temperatures as compared to GSAI and BHAI, indicating that enthalpic contributions to the stability of the hyperthermophilic protein are much greater than the effects of the reduced ΔC_p and changes in ΔS. As a result, the height of the stability curve rises, resulting in an exceptionally stable protein at moderate temperatures as well as an increase in the temperature of thermal unfolding [14,31].

As shown in Table 2, the ΔG_S of TMAI was higher by 19 and 12 kJ/mol than those of BHAI and GSAI, respectively. Despite these changes, the maximal stabilities of the three AIs, where ΔS is zero, occur at similar temperatures (307–310 K). This indicates that entropic and enthalpic contributions to protein stability are similar at the near peak in the stability curve. The above results, therefore, indicate that thermostable AIs owe their thermostability to two mechanisms: One is an upward shift of the entire stability curve to a higher ΔG_U range for TMAI, and the other a reduced ΔC_p for TMAI and GSAI. Divalent metal ions also seem to be very important for the stability of thermophilic AIs, contributing to their lower ΔC_p at elevated temperatures. Interestingly, despite the large differences between their optimal temperatures, the stabilities of these AIs are relatively similar. The ΔG_U values for BHAI, GSAI, and TMAI calculated at their optimum temperatures are 56.7 kJ/mol (50 °C), 45.1 kJ/mol (65 °C), and 40.6 kJ/mol (85 °C), respectively. This suggests that a balance between stability and flexibility is necessary for enzyme function, consistent with the lower activities of TMAI and GSAI at 25 °C. Although, direct comparison of the 3D-structure of these AIs is not yet possible, they can be assumed to be essentially superimposable, as their primary sequences and predicted secondary elements are highly conserved [20]. In view of this, the different thermostabilities are probably due to the small stabilizing features identified in the temperature- and GdnHCl-induced unfolding studies and the protein stability curves presented here.

In conclusion, the present comparative study demonstrates that the holo structure in which the subunits assemble into a tetrameric structure is far more stable than the apo form of AI. Accordingly, the metal-mediated stabilities of both thermophilic proteins displayed shallow temperature dependencies. The increase in conformational rigidity suggests that evolutionary adaptation tends to maintain similar states with respect to conformational flexibility, in that way optimizing biological function under the appropriate physiological conditions. In the light of this, one may infer metal-mediated reduction of ΔC_p to be a powerful method of stabilizing oligomeric proteins at elevated temperatures.

Table 2
Thermodynamic parameters of BHAI, GSAI, and TMAI

Parameters	BHAI		GSAI		TMAI	
	Apo	Holo	Apo	Holo	Apo	Holo
T_m (K)	344	346	350	355	364	373
ΔC_p (kJ/mol K)	33.4 ± 0.3	31.3 ± 0.9	26.5 ± 0.7	22.3 ± 0.3	19.0 ± 0.2	15.2 ± 0.2
ΔH^0_U (kJ/mol)	1286 ± 7	1255 ± 24	1220 ± 19	1122 ± 8	1142 ± 9	1061 ± 8
T_s (K)	307	307	307	308	308	310
ΔG_s (kJ/mol)	69.1	69.4	74.8	76.3	89.1	92.1
ΔS^0 (kJ/mol K)	4.0	4.0	3.8	3.5	3.5	3.2

T_m, ΔH^0 and ΔC_p were determined from fits of the protein stability curves to the Gibbs–Helmholtz equation.

Acknowledgements: This work was supported by Grant AIC-08-02 from Ministry of Commerce, Industry and Energy, Korea. We gratefully acknowledge Prof. Julian Gross for editing the manuscript and Prof. Jerry Eichler for helpful discussions.

References

[1] Jaenicke, R. and Böhm, G. (1998) The stability of proteins in extreme environments. Curr. Opin. Struct. Biol. 8, 738–748.
[2] Adams, M.W.W. and Kelly, R.M. (1998) Finding and using hyperthermophilic enzymes. Trends Biotechnol. 16, 329–332.
[3] Vieille, C. and Zeikus, G.J. (2001) Hyperthermophilic enzymes: sources, uses, and molecular mechanisms for thermostability. Microbiol. Mol. Biol. Rev. 65, 1–43.
[4] Macedo-Ribeiro, S., Darimont, B., Sterner, R. and Huber, R. (1996) Small structural changes account for the high thermostability of 1[4Fe–4S] ferredoxin from the hyperthermophilic bacterium *Thermotoga maritima*. Structure 4, 1291–1301.
[5] Hopfner, K.P., Eichinger, A., Engh, R.A., Laue, F., Ankenbauer, W., Huber, R. and Angerer, B. (1999) Crystal structure of a thermostable type B DNA polymerase from *Thermococcus gorgonarius*. Proc. Natl. Acad. Sci. USA 96, 3600–3605.
[6] Vetriani, C., Maeder, D.L., Tolliday, N., Yip, K.S.P., Stillman, T.J., Britton, K.L., Rice, D., Klum, H.H. and Robb, F.T. (1998) Protein thermostability above 100 °C: a key role for ionic interactions. Proc. Natl. Acad. Sci. USA 95, 12300–12305.
[7] Criswell, A.R., Bae, E.Y., Stec, B., Konisky, J. and Phillips Jr., G.N. (2003) Structures of thermophilic and mesophilic adenylate kinases from the genus *Methanococcus*. J. Mol. Biol. 330, 1087–1099.
[8] Elcock, A.H. (1998) The stability of salt bridges at high temperatures: implications for hyperthermophilic proteins. J. Mol. Biol. 284, 489–502.
[9] Russell, R.J., Ferguson, J.M., Hough, D.W., Danson, M.J. and Taylor, G.L. (1997) The crystal structure of citrate synthase from the hyperthermophilic archaeon *Pyrococcus furiosus* at 1.9 Å resolution. Biochemistry 36, 9983–9994.
[10] Hansen, T., Urbanke, C., Leppänen, V.M., Goldman, A., Brandenburg, K. and Schäfer, G. (1999) The extreme thermostable pyrophosphatase from *Sulfolobus acidocaldarius*: enzymatic and comparative biophysical characterization. Arch. Biochem. Biophys. 363, 135–147.
[11] Ramstein, J., Hervouet, N., Coste, F., Zelwer, C., Oberto, J. and Castaing, B. (2003) Evidence of a thermal unfolding dimeric intermediate for the *Escherichia coli* histone-like HU proteins: thermodynamics and structure. J. Mol. Biol. 331, 101–121.
[12] Li, W.T., Grayling, R.A., Sandman, K., Edmondson, S., Shriver, J.W. and Reeve, J.N. (1998) Thermodynamic stability of archaeal histones. Biochemistry 37, 10563–10572.
[13] Hollien, J. and Marqusee, S. (1999) A thermodynamic comparison of mesophilic and thermophilic ribonucleases H. Biochemistry 38, 3831–3836.
[14] Deutschman, W.A. and Dahlquist, F.W. (2001) Thermodynamic basis for the increased thermostability of CheY from the hyperthermophile *Thermotoga maritima*. Biochemistry 40, 13107–13113.
[15] Bhatt, A.N., Prakash, K., Subramanya, H.S. and Bhakuni, V. (2002) Different unfolding pathways for mesophilic and thermophilic homologues of serine hydroxymethyltransferase. Biochemistry 41, 12115–12123.
[16] Dams, T. and Jaenicke, R. (1999) Stability and folding of dihydrofolate reductase from the hyperthermophilic bacterium *Thermotoga maritima*. Biochemistry 38, 9169–9178.
[17] Panse, V.G., Swaminathan, C.P., Aloor, J.J., Surolia, A. and Varadarajan, R. (2000) Unfolding thermodynamics of the tetrameric chaperone, SecB. Biochemistry 39, 2362–2369.
[18] Backmann, J. and Schafer, G. (2001) Thermodynamic analysis of hyperthermostable oligomeric proteins. Methods Enzymol. 334, 328–342.
[19] Villeret, V., Clantin, B., Tricot, C., Legrain, C., Roovers, M., Stalon, V., Gransdorff, N. and Beeumen, J.V. (1998) The crystal structure of *Pyrococcus furiosus* ornithine carbamoyltransferase reveals a key role for oligomerization in enzyme stability at extremely high temperatures. Proc. Natl. Acad. Sci. USA 95, 2801–2806.
[20] Lee, D.W., Jang, H.J., Choe, E.A., Kim, B.C., Lee, S.J., Kim, S.B., Hong, Y.H. and Pyun, Y.R. (2004) Characterization of a thermostable L-arabinose (D-galactose) isomerase from the hyperthermophilic eubacterium *Thermotoga maritima*. Appl. Environ. Microbiol. 70, 1397–1404.
[21] Lee, D.W., Choe, E.A., Kim, S.B., Eom, S.H., Hong, Y.H., Lee, S.J., Lee, H.S., Lee, D.Y. and Pyun, Y.R. (2005) Distinct metal dependence for catalytic and structural functions in the L-arabinose isomerases from the mesophilic *Bacillus halodurans* and the thermophilic *Geobacillus stearothermophilus*. Arch. Biochem. Biophys. 434, 333–343.
[22] Kim, B.C., Lee, Y.H., Lee, H.S., Lee, D.W., Choe, E.A. and Pyun, Y.R. (2002) Cloning, expression and characterization of L-arabinose isomerase from *Thermotoga neapolitana*: bioconversion of D-galactose to D-tagatose using the enzyme. FEMS Microbiol. Lett. 212, 121–126.
[23] Kim, P. (2004) Current studies on biological tagatose production using L-arabinose isomerase: a review and future perspective. Appl. Microbiol. Biotechnol. 65, 243–249.
[24] Laemmli, U.K. (1970) Cleavage of structural proteins during the assembly of the head of bacteriophage T4. Nature 277, 680–685.
[25] Santoro, M.M. and Bolen, D.W. (1988) Unfolding free energy changes determined by the linear extrapolation method. 1. Unfolding of phenylmethanesulfonyl alpha-chymotrypsin using different denaturants. Biochemistry 27, 8063–8068.
[26] Santoro, M.M. and Bolen, D.W. (1992) A test of the linear extrapolation of unfolding free energy changes over an extended denaturant concentration range. Biochemistry 31, 4901–4907.
[27] Neet, K.E. and Timm, D.E. (1994) Conformational stability of dimeric proteins: quantitative studies by equilibrium denaturation. Protein Sci. 3, 2167–2174.
[28] Zwanzig, R. (1997) Two-state models of protein folding kinetics. Proc. Natl. Acad. Sci. USA 94, 148–150.
[29] Dische, Z. and Borenfreund, E. (1951) A new spectrophotometric method for the detection and determination of keto sugars and trioses. J. Biol. Chem. 192, 583–587.
[30] Myers, J.K., Pace, C.N. and Scholtz, J.M. (1995) Denaturant m values and heat capacity changes: relation to changes in accessible surface areas of protein unfolding. Protein Sci. 4, 2138–2148.
[31] Beadle, B.M., McGovern, S.L., Patera, A. and Shoichet, B.K. (1999) Functional analyses of AmpC beta-lactamase through differential stability. Protein Sci. 8, 1816–1824.